Multicompartmental Particles for Combined Imaging and siRNA Delivery

*Asish C Misra, Srijanani Bhaskar, Nicholas Clay, and Joerg Lahann**

The controlled delivery of genetic material, such as genes, plasmids, or siRNA, holds great promise for the therapy of a number of debilitating diseases.[1–3] While the fundamental concept of permanent or temporary genetic manipulation has been widely embraced by the scientific community, severe concerns remain about the safe and efficient transfer of the genetic material into human cells, where it needs to be released in order to interact with the cell nucleus.[1,2,4] In addition it is desirable, in many cases, to combine gene delivery with a secondary function, such as release of a chemotherapeutic agent or an imaging modality. The main delivery challenges fall broadly into two categories: first, the cell membrane represents an effective barrier against the influx of foreign genetic material resulting in notoriously low transfection rates. Second, a host of nucleases exist in the human body, which cause rapid breakdown of any unprotected genetic material. A number of approaches have been developed to address these challenges including electroporation,[5] viral vectors,[6,7] cationic liposomal formulations,[1] and nanoparticles.[1,2]

While some of these methods have shown moderate to high levels of transfection rates, they are all associated with certain limitations. Electroporation is efficient, but cumbersome and practically limited to *in vitro* applications.[5] The use of viruses can have high efficacy due to evolutionary optimization and is applicable *in vitro* as well as *in vivo*, but comes with substantial safety concerns.[1,2,4,7] If methods other than electroporation or viral vectors are used, macromolecules or particles are generally required for extracellular protection and transport into the cytosol. However, cellular uptake of polymer vehicles involves defined cellular mechanisms, such as receptor-mediated endocytosis.[8] Almost always, the genetic material will then be localized in an endosomal compartment, where it can be deactivated due to abundant nuclease levels and the acidic pH environment.[3,9] Therefore, nanoparticle-based strategies have targeted endosomal escape to overcome liposomal degradation and facilitate release of payload into the cytosol.[1] Positively charged polymers, such as poly(ethylene imine) (PEI),[1] polylysine,[1,2] or cationic acrylate polymers,[10,11] can effectively complex oppositely charged DNA or RNA and are thus well suited for gene delivery. In addition, cationic polymers with large numbers of secondary and ternary amines can act as superabsorbents that expand under the acidic conditions of the endosome and ultimately rupture the ensdosomal compartment physically or osmotically via the "proton sponge" effect.[2,12] This delivery approach has been pursued for nucleic acids[13,14] as well as small molecule drugs.[15,16]

It would however be desirable to combine multiple functions, such as dual release of genetic material and cytostatic drugs, or release and simultaneous imaging of the particles to monitor intracellular particle fate.[17–19] While the highly charged nature of cationic polymers has been successfully utilized to complex oppositely charged DNA or RNA fragments, incorporation of additional functional moieties with different chemical properties is more difficult generally requiring fairly sophisticated chemical conjugation techniques.[20–23] In principle, this could be achieved by using a combination of two different types of nanoparticles: one made of a cationic polymers to enable endosomal escape and intercellular delivery of the genetic material, and a second one to provide the an additional imaging functionality. However, if a mixture of two independent particles is used, the fate of the particles is not necessarily coupled, and prevalence of one type of particle over the other is likely, at least for specific anatomical sites. Moreover, instead of the desirable synergistic effects, separate particles may actually compete for cellular uptake due to the finite endocytic uptake capacity of the target cells.[24–26] The herein proposed approach employs multifaceted polymer nanoparticles that enable DNA loading and inclusion of imaging modalities on the same particle, although in two distinct compartments.

Emerging evidence in our laboratory on electrohydrodynamic co-jetting[27] suggests that the synthesis of multicompartmental particles with substantially dissimilar compartments is feasible.[28–30] Electrohydrodynamic co-jetting is based on the laminar flow of two or more polymer solutions through a capillary nozzle.[31] As shown in **Figure 1**a, two (or more) polymer solutions are extruded through 26G needles in a laminar flow regime, and hence there is minimal mixing at the tip of the needle where the droplet forms. The use of high electrical fields ensures formation of a jet at the tip of the distorted droplet

A. C. Misra, Prof. J. Lahann
Department of Biomedical Engineering
The University of Michigan
2300 Hayward St., Ann Arbor, MI 48109, USA
E-mail: lahann@umich.edu
Dr. S. Bhaskar, Prof. J. Lahann
Department of Macromolecular Science and Engineering
The University of Michigan
2300 Hayward St., Ann Arbor, MI 48109, USA
Dr. N. Clay, Prof. J. Lahann
Department of Chemical Engineering
3414 GGBL2300 Hayward, Ann Arbor, MI 4809, USA
Prof. J. Lahann
Department of Materials Science and Engineering
The University of Michigan
2300 Hayward St., Ann Arbor, MI 48109, USA
A. C. Misra
The University of Michigan Medical School
2300 Hayward St., Ann Arbor, MI 48109, USA

DOI: 10.1002/adma.201200372

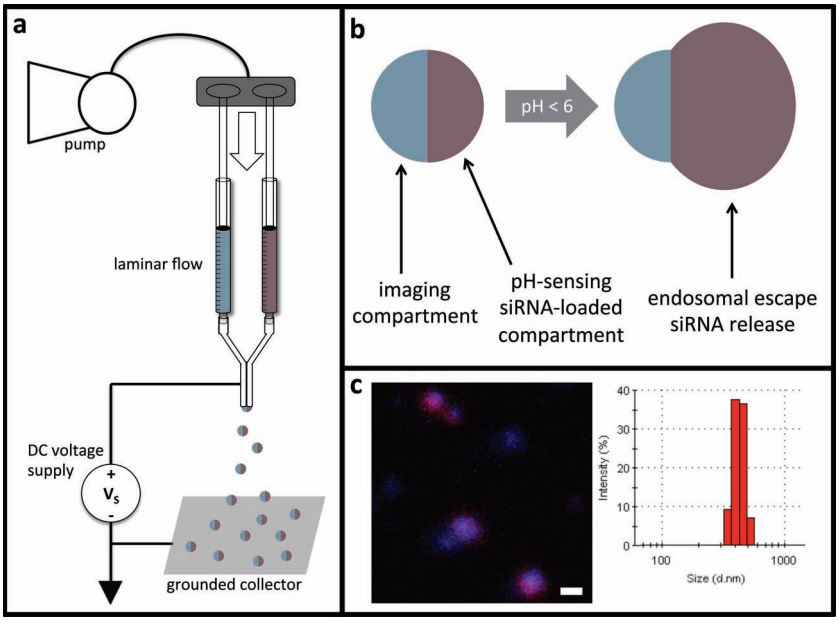

Figure 1. (a) Scheme representing the electrohydrodynamic co-jetting process for fabrication of bicompartmental particles. (b) Bicompartmental particle design showing dissimilar compartments with complementary functions–imaging and siRNA delivery (and endosomal escape). (c) Representative fluorescent CLSM and SEM images of siRNA-loaded bicompartmental nanoparticles (scale bars are 1 μm).

formed at the end of the nozzle, the so-called Taylor cone. The formation of the Taylor cone is due to the balance of three forces acting on a droplet at the tip of the syringes–surface tension, gravity, and an electric force resulting from the electric field generated by the DC voltage.[32] Because of the high jet velocities, thinning of the polymer thread by several orders of magnitude induces virtually instantaneous solvent evaporation, which, in turn, leads to ultrafast nanoprecipitation, resulting in droplets or a fiber in accordance with Rayleigh instability.[33] Under the conditions of electrohydrodynamic co-jetting, particles can be prepared that mirror the compartmentalized flow initially induced under the laminar flow regimen of the capillary nozzles. Variation of the processing parameters has produced different shapes, from spheres to rods and disks.[34] In addition to particles, a slightly modified approach can yield multicompartmental fibers.[31,35] The resulting fibers can be further sectioned into microcylinders with defined aspect ratios.[36] This approach has been successfully applied to water-borne[27,37] as well as organic polymer[34,36] solutions. The use of additives in the respective jetting solutions, such as polymers,[38] dyes,[27,28,31,34–37] small molecule drugs, or even nanocrystals,[39,40] leads to selective loading of certain particle compartments.

We now propose to use electrohydrodynamic co-jetting to prepare orthogonal particle architectures with two substantially different compartments for combined imaging and release, i.e., (i) a hydrogel-based release compartment (hydrophilic) and (ii) an imaging compartment (hydrophobic). The hydrophobic compartment consists of poly(DL-lactide-co-glycolic acid) [PLGA], which is suitable for loading of fluorescent dyes or nanoparticles, such as iron oxide nanocrystals.[39,40] This additional functionality can enable monitoring of particle fate during delivery *in vitro* and *in vivo*. PLGA may also be used to load complementary therapeutics, such as doxorubicin.[41–43] In contrast, the hydrogel compartment consists of polyethyleneimine (PEI) (as well as a small amount of PLGA), a cationic polymer that is highly water adsorbent.[44] At lower pH values, the primary amines of the PEI are protonated and undergo electrostatic repulsion. Macroscopically, this causes the hydrogel to swell.[45] Because the endosomes of mammalian cells are generally at lower pH levels than the physiological blood pH level of around 7.4, the PEI hydrogel compartment can be used to "detect" the acidic pH of the endosome, once it enters via endocytosis. It then swells, thereby either mechanically breaking the endosome, or inducing osmotic bursting. Additionally, due to PEI's cationic nature, it is suitable for complexation of nucleic acids (due to their anionic character). As shown in Figure 1b and Figure 1c, we designed and prepared multicompartmental nanoparticles employing the PLGA compartment as an imaging modality, and the PEI compartment as an endosome sensing and escape compartment that also serves as a siRNA release compartment. The imaging compartment is labeled with a blue fluorescent polymer dye that remains in the compartment throughout the release study. In contrast, the hydrogel compartment contains the siRNA-payload along with a transient red fluorescent dye (Figure 1c). The nanoparticles are displayed in Figure 1c and feature uniform sizes and shapes.

To characterize the compartmentalization of these particles, the size of the particles had to be increased in order to visualize the particles by confocal microscopy. Crosslinking of the PEI compartment was achieved via incorporation of dithiobis(succinimidyl propionate) (DSP), a small molecule consisting of two N-hydroxysuccinimide esters, which are reactive to amines. The swelling behavior of the PLGA/PEI particles in various buffered aqueous solutions was controlled by modifying critical jetting parameters including molecular weight or incorporation of crosslinker into the PEI jetting solution. The use of a higher molecular weight PEI resulted in a higher degree of swelling of the particles after electrohydrodynamic co-jetting (**Figure 2**a). Because equimolar amounts of crosslinker were used for both polymers, the relative crosslinking density of the lower molecular weight PEI was increased relative to the high-molecular weight PEI. Hence, the high molecular weight PEI was associated with a higher swelling capacity, as shown in Figure 2a. Because of this higher swelling capacity, all further experiments were conducted with the high molecular weight PEI.

Moreover, in the absence of crosslinker, swelling was faster and complete dissolution of the compartment in water was observed eventually. In contrast, crosslinked particles swelled less and remained stable in their swollen state (Figure 2b). This observation implies that for an uncrosslinked PEI compartment, the particle can enter a cell's endosome with minimal release

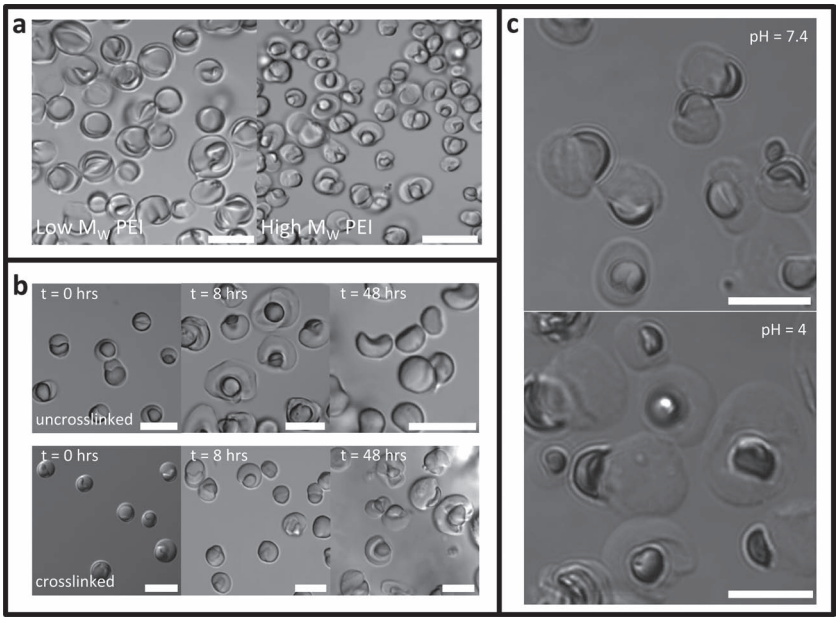

Figure 2. Swelling studies performed via DIC microscopy. Particles incorporating higher molecular weight PEI exhibit a higher degree of swelling after four hours in PBS (a). Particles incorporating uncrosslinked PEI are observed to have different swelling kinetics than that of crosslinked PEI, as well as eventually having complete dissolution of the PEI (b). Particles with crosslinked PEI show different degrees of swelling at different pH levels after 6 hours of incubation in the appropriate buffered solutions (c). All scale bars are 10 μm.

of small molecule drugs, as little swelling is observed initially (Figure 2b, uncrosslinked). After 8 hours, a swollen PEI compartment is observed clearly intact (Figure 2b, uncrosslinked), implying that endosomal escape is possible. Given the timeframe of particle uptake being four to six hours,[46] the particles should have enough time to enter cells and escape endosomes. Subsequently siRNA can then be released completely into the cytosol after 48 hours due to complete dissolution of PEI by that time (Figure 2b, uncrosslinked).

After the particles have been prepared, the crosslinking reactions between the NHS ester groups in the crosslinker and amines in the PEI can continue for a certain period in the solid state. Because we ultimately intend to use these particles for *in vitro* delivery of siRNA, it is critical that the particles were prepared as stable formulations with predictable mechanical and chemical properties. One prerequisite was therefore that the crosslinking was completed before cells were allowed to be in contact with the particles. We thus conducted a detailed IR spectroscopy analysis. To facilitate IR spectroscopy, the particles were deposited as a thin film onto a gold-coated silicon substrate. By monitoring the loss of the peak at 1760 cm^{-1} (ester groups) and the growing peak at 1660 cm^{-1} (formation of new amide bonds), we determined that the crosslinking reaction indeed proceeds in the bulk for more than a day and then ceased after 48 hours (Figure S3). Based on this finding, the particles were routinely dried in air or under vacuum dessication for at least 48 hours prior to conducting further experiments.

With these fully crosslinked particles in hand, we then conducted a set of swelling experiments in phosphate buffered saline (pH = 7.4) and an aqueous acetic acid and sodium acetate buffered solution (pH = 4). As shown in Figure 2c, the PEI compartment was substantially more swollen at pH = 4 than at pH = 7.4 (Figure 2c). In either buffer, we observed that the bicompartmental nature of the particles was maintained as the hydrophobic PLGA compartment was clearly delineated from the hydrogel PEI hemisphere. As expected, the PLGA side did not change in either buffer, unlike the PEI compartment (Figure 2c), which had become substantially larger. These results are shown for a PLGA/PEI compartment with 1:1 w/w PLGA:PEI, using 60 kDa (high molecular weight) PEI with 5 wt% DSP with respect to the amount of PEI. We note that the swelling rate and size of the swollen compartment can be controlled by varying the aforementioned parameters providing adequate control over the final particle sizes.

In addition to achieving tight control over the swelling behavior, we were also interested to prepare a number of other compartment geometries beyond Janus particles, which may be important in future work, when incorporation of small molecule drugs will be combined with gene delivery. To demonstrate as a proof of concept, tetracompartmental particles were fabricated, which were comprised of two hydrophobic compartments and two hydrogel compartments (Figure S1). These particles were made from a nozzle with four capillaries. The two opposing capillaries contained either PLGA only, or a blend of PLGA and PEI. The second PLGA compartment could be used to incorporate a small molecule drug. The additional hydrogel compartment might for instance be used to incorporate a second type of siRNA. Independent control of the release rates can then be simply tailored by altering the amount of hydrogel and/or crosslinker in the two compartments.

Next, the particle swelling and release kinetics were assessed by selectively loading rhodamine-labeled siRNA into the PEI compartment. The particles reached the maximum swelling within 15 hours at pH 7.4, and maintained their dimensions thereafter (**Figure 3**a). Hence, if the particles were only placed in aqueous solution immediately before incubation with cells, as it was the case in the following experiments, minimal swelling can be expected to occur prior to endosomal uptake into the cells.[46] In contrast, significant swelling will occur at the lower pH after entering an endosome; ultimately breaking the endosomes either physically or by osmotic pressure.

Figure 3b and 3c demonstrate the compartmentalization and release of rhodamine-labeled siRNA at a pH of 7.4. Despite siRNA having a relatively low molecular weight, we observe that the there is a clear interface between the compartment with siRNA and blue fluorescent imaging compartment. This well-defined interface, as well as the 50% release of the total siRNA loaded, may partially be attributed to the fact that the siRNA is tightly complexed with the PEI due to strong electrostatic interactions.

To assess the *in vitro* uptake and efficacy of PLGA/PEI particles loaded with siRNA (PLGA/PEI-siRNA), we decreased the

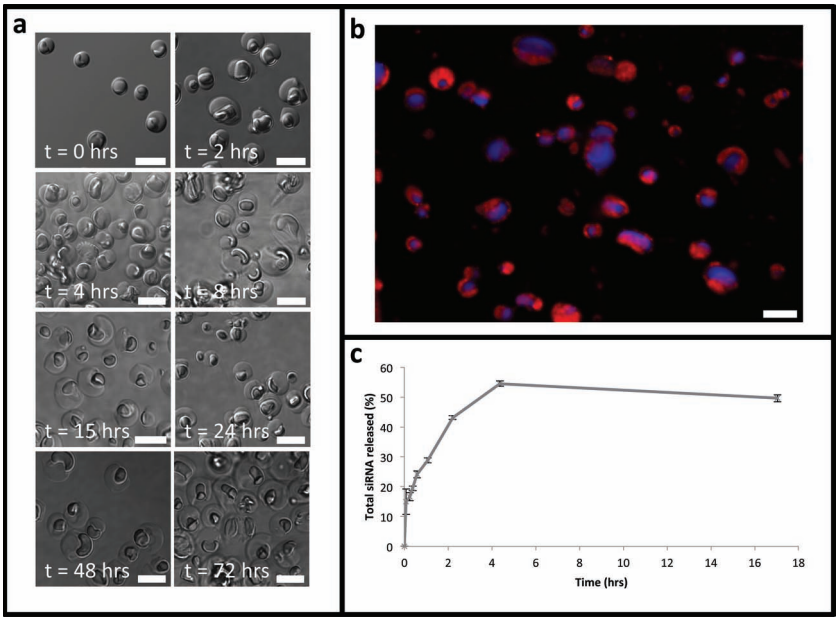

Figure 3. Swelling kinetics of bicomparmental particles with crosslinked high M_W PEI via DIC microscopy (a). Fluorescent CLSM image of bicomparmental particles, with blue fluorescent PLGA imaging compartment, and a composite PLGA/crosslinked PEI compartment loaded with rhodamine-labeled siRNA (b). Release kinetics (c) of siRNA from particles (b), done in PBS. All scale bars are 10 μm.

particle size to an average of about 216 nm, with a 95% confidence interval between 203 and 219 nm (Figure S6). A representative subpopulation of these particles is shown in Figure 1c. To ensure maximum levels of delivery of siRNA, no crosslinker was used in these particles. Hence, these uncrosslinked particles should deliver their entire siRNA payload within 48 hours, when the particles are completely disolved (Figure 2b). We employed a GFP expressing epithelial breast cancer line, MDA-MB-231/GFP, and used an siRNA against GFP to assess the therapeutic efficacy of siRNA delivery using the PLGA/PEI-siRNA particles. Using the imaging modality provided by the PLGA compartment, we were able to demonstrate that the particles are uptaken readily by the MDA-MB-231/GFP cells (Figure S4). Particles were incubated overnight with cells seeded on a 12-well plate; subsequent confocal imaging demonstrated a high level of blue fluorescence from the imaging compartment of the particles co-localized with green fluorescence emanating from the GFP expressing MDA-MB-231/GFP cells (Figure S4), confirming particle uptake.

We further assessed the efficacy of the PLGA/PEI-siRNA nanoparticles in terms of GFP silencing in a dose-response experiment. As shown in **Figures 4** and **5**, the particles were able to silence GFP production within 2 days, which again coincided with the complete dissolution of the PEI compartments. When soluble siRNA was placed in the media, PLGA/PEI nanoparticles did not cause uptake of this siRNA (second row of Figure 4); only PLGA/PEI-siRNA nanoparticles (i.e., particles loaded with siRNA) resulted in silencing of GFP (third row of Figure 4). This confirms that the particles are indeed taken up and siRNA is released in the cytosol, as opposed to siRNA entering the cells from the outside environment via unspecific pathways. It might be hypothesized that PEI used at higher concentration may destabilize cell membranes and thus enhanced uptake.[47] Therefore, a control experiment was included, where PLG/PEI without siRNA loading were prepared and then delivered to the cells together with spiked-in, free siRNA. If there is membrane damage caused by the particles, the free siRNA should be able to enter the cytosol and silence the GFP expression. Based on our control experiment, this, however, is not the case. The data shown in Figure 4 clearly demonstrate that siRNA is not entering via this method, but rather through endocytosis-mediated uptake of particles loaded with siRNA. Finally, the toxicity of the particles was assessed by XTT assay (Figure S5). The results indicated that the toxicity of the bicompartmental particles can be neglected up to concentrations of at least 100 μg/mL. Taken together, bicompartmental particles at a concentration of 100 μg/mL is not only nontoxic, but also effective at silencing GFP expression.

The GFP silencing was then quantified by image analysis. We observed GFP silencing in response to incubation with PLGA/PEI-siRNA particles, while cells incubated with PLGA/PEI particles or PLGA/PEI particles with soluble siRNA (PLGA/PEI+siRNA) did not show reduced GFP expression (Figure 5). We also observed a dose-dependent silencing response–incubation with a lower concentration of PLGA/PEI-siRNA particles (50 μg/mL) resulted in lower silencing of GFP–on days 2, 3, and 4, we observed GFP expression of approximately 16.94 ± 0.94, 18.69 ± 1.35, and 24.17 ± 3.04, respectively–these values are all consistently higher than those of GFP expression from cells incubated with PLGA/PEI-siRNA particles at a concentration of 100 μg/mL). Additional controls were performed, such as incubation of cells only with siRNA, which, as expected, was not taken up and no GFP silencing was therefore observed. The positive control of PEI complexed with siRNA was expected to perform superior with respect to GFP silencing, as the amount of siRNA used was about two orders of magnitude higher than that used in the particles. We selected the lower siRNA levels in the Janus particles to mirror the concentrations used in other published studies.[48,49] However, it is important to note that the control PEI-siRNA complexes only had about a third more reduction in GFP as compared to the PLGA/PEI particles, in spite of the fact that they had about two orders of magnitude less siRNA. These findings suggest that our new particles have a higher transfection efficiency than what was observed with the standard PEI transfection method.

In conclusion, we have produced nanoparticles with two dissimilar compartments. These novel particles allow for incorporation of dual imaging and siRNA release functions. The electrohydrodynamic co-jetting approach used to prepare these particles features independent choice of the chemical composition for the two individual compartments. This was then used to control the degree of swelling as well as the amount of siRNA released in a given period. The pH-sensitive PEI compartment

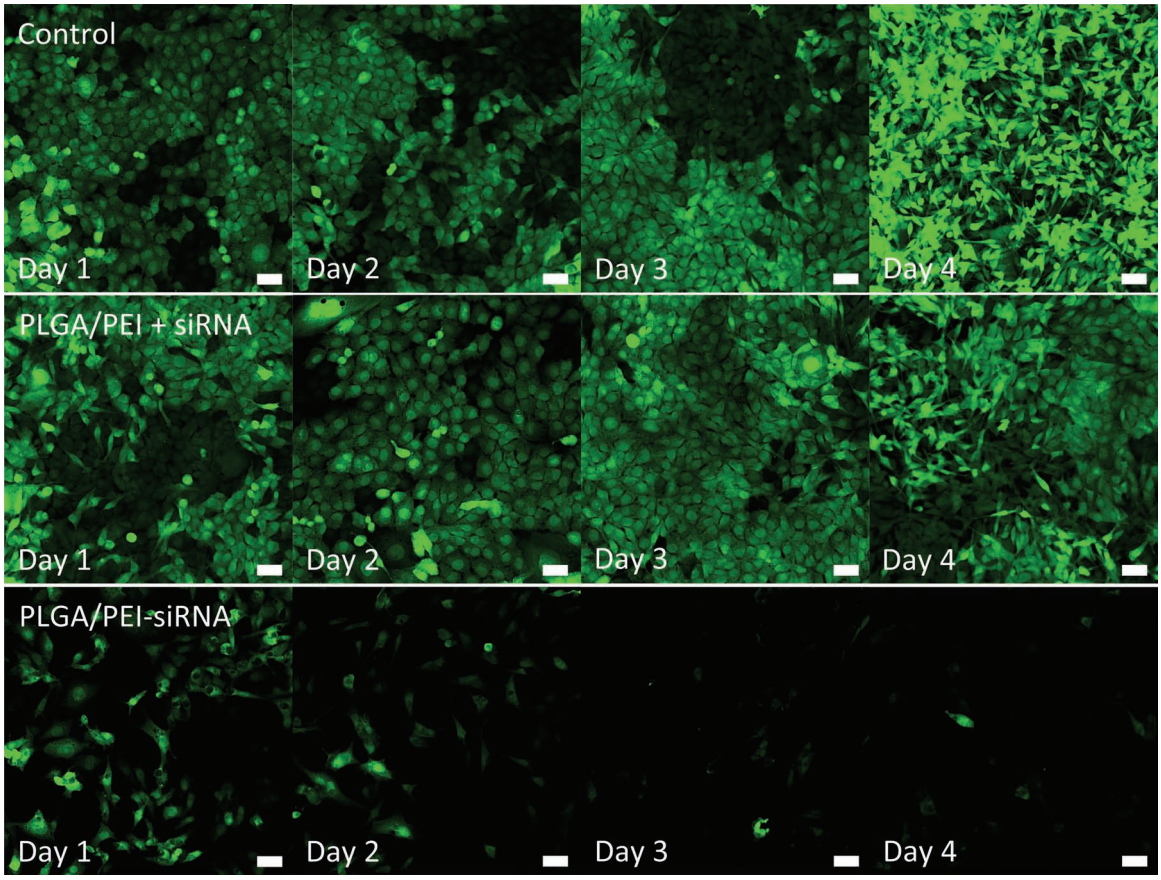

Figure 4. *In vitro* particles incubation experiments with MDA-MB-231/GFP breast cancer cells. First row shows cells with no particle or siRNA treatment. Second row (PLGA/PEI + siRNA) shows results from incubating particles and soluble siRNA (not loaded in the particles). Third row (PLGA/PEI-siRNA) shows results from incubation with siRNA-loaded particles. All scale bars are 50 µm. Concentrations for the particles shown here were 100 µg/mL.

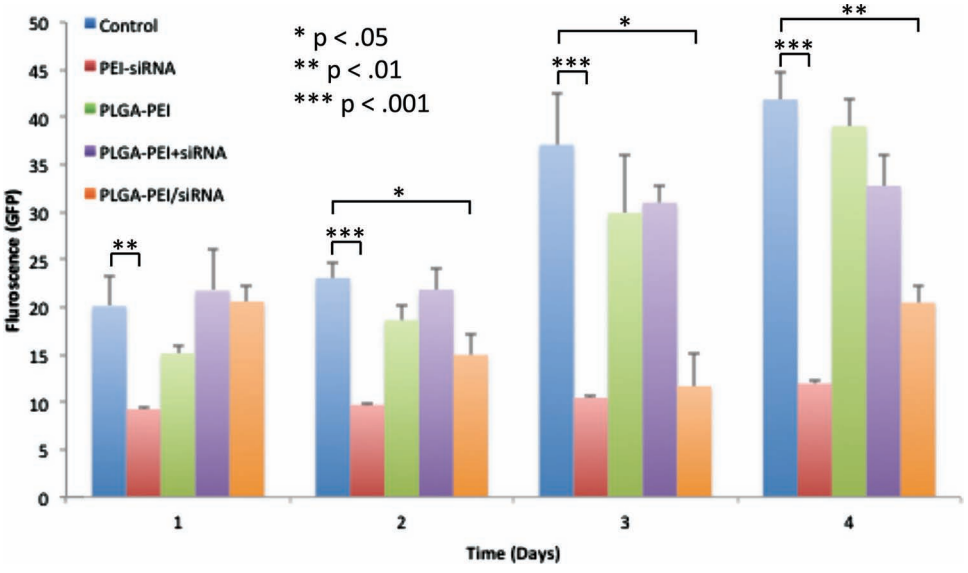

Figure 5. Quantification of GFP expression by image analysis. Control represents cells that have not been incubated with particles nor siRNA. PEI-siRNA represents a control where cells were incubated with PEI-siRNA polyplexes (1 mg/mL PEG, 1 µg/mL siRNA). PLGA/PEI+siRNA represents cells incubated with bicompartmental particles and soluble siRNA (100 µg/mL PLGA/PEI, 1 µg/mL siRNA). PLGA/PEI-siRNA represent cells incubated with siRNA-loaded bicompartmental particles at a concentration of 100 µg/mL.

allows sensing of the endosomal environment, further swelling and bursting out of the endosome, thereby releasing the siRNA in the cytosol, where it can be biologically active. Finally, we assessed the *in vitro* efficacy of the particles to silence GFP expression in MDA-MB-231/GFP using an anti-GFP siRNA. The siRNA-loaded particles were able to silence GFP at a level comparable to our positive control, PEI-siRNA complexes, however, using two orders of magnitude lower amounts of siRNA. These nanocarriers have the potential to serve as delivery vectors for multiple drugs as well as gene delivery, allowing for synergistic effects, which are known to be effective in combating disease such as cancer.[50,51] Additionally, the potential of "theranostics"

maybe achieved through these particles as imaging modalities may be incorporated. Manufacturing nanoparticles with multiple compartments could provide multiple functionalities that otherwise could not be incorporated into the same particle, allowing for a wide array of possible applications.

Experimental Section

Materials: Poly(DL-lactide-co-glycolic acid) [50–75 kg/mol], polyethyleneimine (60 kg/mol), blue fluorescent poly[(*m*-phenylenevinylene)-alt-(2,5-dihexyloxy-*p*-phenylenevinylene)] (PMPDHPV), and all solvents were purchased from Sigma. Dithiobis(succinimidyl propionate) [DSP] and paraformaldehyde were obtained from Thermo Scientific. Red fluorescent polythiophene polymer ADS306PT was purchased from American Dye Source, Inc. Small interfering RNAs against GFP (both tagged with rhodamine and untagged) were purchased from Qiagen. MDA-MB-231/GFP cells were purchased from Cell Biolabs. All cell culture materials, including Dulbecco's Modified Eagle Medium (DMEM), fetal bovine serum (FBS), non-essential amino acids, and penicillin-streptomycin, were obtained from Gibco. XTT reagents were purchased from Invitrogen.

Fabrication of multicompartmental particles: PLGA/PEI and PLGA/PEI-siRNA particles were produced via electrohydrodynamic co-jetting.[34] When dyes (PMPDHPV and ADS306PT) were incorporated into the jetting solutions, they were used at concentrations less than or equal to .01 w/v%. Generally, 5 w/v% polymer solutions were used for both sides, with the PLGA/PEI side having either 50:50 w/w PLGA:PEI (for characterization), or 4:1 w/w PLGA:PEI (for *in vitro* testing). A mixture of chloroform ($CHCl_3$) and N,N-dimethylformamide (DMF) was used as the solvent–97:3 v/v $CHCl_3$:DMF was used for particles fabricated for characterization, while for the particles used in *in vitro* studies, 50:50 v/v $CHCl_3$:DMF was used. When DSP was used as a crosslinking agent, it was incorporated into the PEI jetting solution in the amount of 5 wt% with respect to the amount of PEI. To incorporate siRNA, it was first complexed with PEI in water, lyophilized, and then dissolved in the jetting solvent, along with PLGA (and DSP). 80 ng of siRNA were incorporated into the solution for every 1 mg of polymeric material, resulting in an siRNA loading of 80 ng siRNA/mg particle.

Particle characterization: To confirm the bicompartmental character, polymeric dyes were used, as well as rhodamine labeled siRNA, and fluorescence imaging was done using an Olympus FluoView 500 Laser Scanning Confocal Microscope (CLSM). Differential interference contrast microscopy (DIC) for swelling studies was performed using the same CLSM microscope. Scanning electron micrographs were obtained using an AMRAY 1910 Field Emission Scanning Electron Microscope (FEG-SEM). Particle size was determined by analysis of SEM images via Image J.

Cell culture: MDA-MB-231/GFP cells were cultured in DMEM with high glucose and glutamine, supplemented with 10% FBS, 1X non-essential amino acids, and 1X penicillin-streptomycin. Passaging was performed by washing the cells once with Dulbecco's phosphate buffered saline (D-PBS), incubating with 0.25% trypsin for 5–10 minutes, subsequently diluting with media, centrifuging the cells, and finally seeding in flasks or well plates.

GFP silencing experiments: Cells were seeded at 25000 cells/well in a 12-well plate with circular glass slides. After one day, particles and siRNA were incubated overnight (~12 hours). Media was changed every day, and cells were fixed 1, 2, 3, and 4 days after particle incubation. Cell fixing was performed by washing the cells with D-PBS and incubating with paraformaldehyde for 30 minutes. Cells were washed once more with D-PBS, and the glass slides were then removed and mounted using ProLong Gold with DAPI. Slides were imaged using fluorescence microscopy using the same laser power settings for each channel and each sample. GFP expression was quantified using Image J to analyze the GFP channel from the images. Statistical significance was set at $p < 0.05$.

XTT Assay: Cytotoxicity of particles was assessed by incubating varying concentrations of particles with cells seeded on a 96-well plate at a concentration of 5000 cells/well. Particles were incubated with cells for 24 hours, and XTT assay was performed as per protocol provided by Invitrogen with the XTT assay kit.

Supporting Information

Supporting Information is available from the Wiley Online Library or from the author.

Acknowledgements

The authors thank the American Cancer Society (RSG–08–284–01–CDD) for financial support. Special thanks to Sahar Rahmani, Jaewon Yoon, and Thomas Eyster for valuable discussions about data, experimental methods, and editing of the manuscript.

Received: January 26, 2012
Revised: February 28, 2012
Published online: May 14, 2012

[1] M. A. Mintzer, E. E. Simanek, *Chem. Rev.* **2009**, *109*, 2.
[2] D. W. Pack, A. S. Hoffman, S. Pun, P. S. Stayton, *Nat. Rev. Drug Disc.* **2005**, *4*, 7.
[3] K. A. Whitehead, R. Langer, D. G. Anderson, *Nat. Rev. Drug Disc.* **2009**, *8*, 2.
[4] T. Niidome, L. Huang, *Gene Therapy* **2002**, *9*, 24.
[5] S. Somiari, J. Glasspool-Malone, J. J. Drabick, R. A. Gilbert, R. Heller, M. J. Jaroszeski, R. W. Malone, *Mol. Therapy* **2000**, *2*, 3.
[6] K. J. Fisher, K. Jooss, J. Alston, Y. Yang, S. E. Haecker, K. High, R. Pathak, S. E. Raper, J. M. Wilson, *Nat. Med.* **1997**, *3*, 3.
[7] M. A. Kay, J. C. Glorioso, L. Naldini, *Nat. Med.* **2001**, *7*, 1.
[8] S. D. Conner, S. L. Schmid, *Nature* **2003**, *422*, 6927.
[9] L. Hu, Z. W. Mao, C. Y. Gao, *J. Mater. Chem.* **2009**, *19*, 20.
[10] C. Zhu, S. Jung, S. Luo, F. Meng, X. Zhu, T. G. Park, Z. Zhong, *Biomaterials* **2010**, *31*, 8.
[11] J. O. You, D. T. Auguste, *Biomaterials* **2010**, *31*, 26.
[12] A. Akinc, M. Thomas, A. M. Klibanov, R. Langer, *J. Gene Med.* **2005**, *7*, 5.
[13] O. Boussif, F. Lezoualc'h, M. A. Zanta, M. D. Mergny, D. Scherman, B. Demeneix, J. P. Behr, *PNAS* **1995**, *92*, 16.
[14] W. T. Godbey, K. K. Wu, A. G. Mikos, *J. Controlled Release* **1999**, *60*, 2–3.
[15] S. V. Vinogradov, E. Kohli, A. D. Zeman, *Pharm. Res.* **2006**, *23*, 5.
[16] T. K. Bronich, S. V. Vinogradov, A. V. Kabanov, *Nano Letters* **2001**, *1*, 10.
[17] S. Santra, C. Kaittanis, J. Grimm, J. M. Perez, *Small* **2009**, *5*, 16.
[18] V. Bagalkot, L. Zhang, E. Levy-Nissenbaum, S. Jon, P. W. Kantoff, R. Langer, O. C. Farokhzad, *Nano Letters* **2007**, *7*, 10.
[19] C. Loo, A. Lowery, N. Halas, J. West, R. Drezek, *Nano Letters* **2005**, *5*, 4.
[20] S. Moffatt, S. Wiehle, R. J. Cristiano, *Gene Therapy* **2006**, *13*, 21.
[21] J. A. Hubbell, *Gene Therapy* **2006**, *13*, 19.
[22] S. Boeckle, J. Fahrmeir, W. Roedl, M. Ogris, E. Wagner, *J. Controlled Release* **2006**, *112*, 2.
[23] E. Wagner, *Pharm. Res.* **2004**, *21*, 1.
[24] M. P. Desai, V. Labhasetwar, E. Walter, R. J. Levy, G. L. Amidon, *Pharm. Res.* **1997**, *14*, 11.
[25] M. S. Cartiera, K. M. Johnson, V. Rajendran, M. J. Caplan, W. M. Saltzman, *Biomaterials* **2009**, *30*, 14.

[26] K. Y. Win, S. S. Feng, *Biomaterials* **2005**, *26*, 15.
[27] K. H. Roh, D. C. Martin, J. Lahann, *Nat. Mater.* **2005**, *4*, 10.
[28] J. Lahann, *Small* **2011**, *7*, 9.
[29] J. Yoon, K. J. Lee, J. Lahann, *J. Mater. Chem.* **2011**, *21*, 24.
[30] K. J. Lee, J. Yoon, J. Lahann, *Curr. Op. Coll. & Inter. Sci.* **2011**, *16*, 3.
[31] S. Bhaskar, J. Lahann, *J. Am. Chem. Soc.* **2009**, *131*, 19.
[32] A. M. Ganan-Calvo, *Phys. Rev. Letters* **1997**, *79*, 2.
[33] W. D. Luedtke, U. Landman, Y.-H. Chiu, D. J. Levandier, R. A. Dressler, S. Sok, M. S. Gordon, *J. Phys. Chem. A* **2008**, *112*, 40.
[34] S. Bhaskar, K. M. Pollock, M. Yoshida, J. Lahann, *Small* **2010**, *6*, 3.
[35] S. Mandal, S. Bhaskar, J. Lahann, *Macromol. Rapid Comm.* **2009**, *30*, 19.
[36] S. Bhaskar, J. Hitt, S.-W. L. Chang, J. Lahann, *Angew. Chem. Int. Ed.* **2009**, *48*, 25.
[37] K. H. Roh, D. C. Martin, J. Lahann, *J. Am. Chem. Soc.* **2006**, *128*, 21.
[38] K. J. Lee, S. Hwang, J. Yoon, S. Bhaskar, T.-H. Park, J. Lahann, *Macromol. Rapid Comm.* **2011**, *32*, 5.
[39] D. W. Lim, S. Hwang, O. Uzun, F. Stellacci, J. Lahann, *Macromol. Rapid Comm.* **2010**, *31*, 2.
[40] S. Hwang, K.-H. Roh, D. W. Lim, G. Wang, C. Uher, J. Lahann, *Phys. Chem. Chem. Phys.* **2010**, *12*, 38.
[41] T. Govender, S. Stolnik, M. C. Garnett, L. Illum, S. S. Davis, *J. Controlled Release* **1999**, *57*, 2.
[42] R. Lin, L. Ng, C.-H. Wang, *Biomaterials* **2005**, *26*, 21.
[43] T. Betancourt, B. Brown, L. Brannon-Peppas, *Nanomedicine* **2007**, *2*, 2.
[44] J. Suh, H. J. Paik, B. K. Hwang, *Bioorg. Chem.* **1994**, *22*, 3.
[45] J. P. Behr, *Chimia* **1997**, *51*, 1–2.
[46] J. Panyam, V. Labhasetwar, *Pharm. Res.* **2003**, *20*, 2.
[47] H. Lv, S. Zhang, B. Wang, S. Cui, J. Yan, *J. Controlled Release* **2006**, *114*, 1.
[48] A. Zintchenko, A. Philipp, A. Dehshahri, E. Wagner, *Bioconjug. Chem.* **2008**, *19*, 7.
[49] M. Thomas, Q. Ge, J. J. Lu, J. Chen, A. Klibanov, *Pharm. Res.* **2005**, *22*, 3.
[50] A. Goldin, N. Mantel, *Cancer Res.* **1957**, *17*, 7.
[51] T. C. Chou, *Cancer Res.* **2010**, *70*, 2.